Flexural Performance of PVA Reinforced ECC Beams: Numerical and Parametric Studies

Hind Mahmood Khudhur[a], Mustafa Özakça[a], Abdolbaqi Mohammed Khdher[b,*],Talha Ekmekyapar [a]
[a] Department of Civil Engineering
University of Gaziantep
27310 Gaziantep, Turkey
[b] Faculty of Mechanical Engineering,
University Malaysia Pahang,
26600 Pekan, Pahang, Malaysia

* Corresponding author E-mail address: abdolbaqi.mk@gmail.com

Abstract—Engineered cementitious composite (ECC) refers to the group of cementitious mixtures possessing the strain-hardening and crack control abilities. In this research, the mechanical performance of ECC beams will be investigated with respect to the effect of aggregate size and amount, by employing nonlinear finite element method. The validity of the models were verified with the experimental results of the ECC beams under monotonic loading. Based on the numerical analysis method, nonlinear parametric study was then conducted to evaluate the influences of various parameters on the flexural stress and flexural deflection of ECC beams. A new models that accounts for the ECC aggregate content (*AC*), ECC compressive strength (f_{ECC}), and maximum aggregate size (D_{max}) parameters are proposed. The analytical results obtained from the proposed models were compared with experimental results obtained from 57 ECC beam tests previously published. The simulation results indicated that when increase the aggregate size and content no definite trend in flexural strength is observed and the ductility of ECC is negatively influenced by the increase of aggregate size and content. Also, the ECC beams revealed enhancement in terms of flexural stress, strain, and midspan deflection when compared with the reference beam (microsilica MSC), where, the average improvement percentage of the specimens were 45%, 1242%, and 1427.15%, respectively. These results are quite similar to that of the experimental results, which provides that the finite element model is in accordance with the desirable flexural behaviour of the ECC beams. Furthermore, the proposed models can be used to predict the flexural behaviour of ECC beams with great accuracy.

Keywords—engineered cementitious composite (ECC); flexural behavior; ductility; finite element modelling; parametric study

1. Introduction

Concrete is a quasi-brittle material. When its tensile strength is reached, a single crack forms and the crack width increases indefinitely. Even with steel reinforcements, crack width control in structures often proves unreliable. Because cracking in structures reduces durability by allowing easy penetration of aggressive chemical agents into the concrete cover, many attempts have been made to overcome the quasi-brittle nature of concrete [1]. Recently, engineered cementitious composites (ECCs) have been proposed as a new class of concrete materials which have considerably greater level of ductility. ECC is a unique kind of cementitious composite having high ductility and damage tolerance properties under intense mechanical loadings, including tensile and shear loadings. The material is optimized as per the principles of micromechanics which increases the tensile strain capacity of material up to 3-5% where operating uniaxial tensile loading making it achievable through only 2% polyvinyl alcohol (PVA) or polyethylene fibre (PE) quantity by volume [2-5]. The characteristic strain-

hardening behavior of ECC is accompanied by the sequential development of multiple microcracking. Even at ultimate load, the crack width remains on the order of 50 to 80 μm.

A micromechanics-based material design theory is employed to enhance the strength and energy ratios of the mixture proportions of ECC to acquire high composite ductility [2, 6, 7]. The crack control properties of ECCs with respect to controlling the width of occurring cracks depend upon the type, size, and amount of fibre, matrix ingredients and interface properties of the material. The manufacture of ECCs is done by employing particular quantities of high-quality mixtures, which when accompanied by the bristly material in the paste, helps to enhance the matrix (ECC without fibre) toughness. As a result, the material attains the crack control characteristics i.e. delayed crack initiation and prevention of steady-state flat-crack propagation which might cause to reduce the tensile ductility of ECC. Moreover, the introduction of aggregates with a particle size larger than the average fiber spacing leads to balling of fibers and results in poor fiber dispersion uniformity [8, 9]. This proposes that ECC with fine aggregate must have a standard aggregate/binder ratio (A/B) of 0.36 and a maximum grain size of 250 μm [5, 10].

Due to environmental and economical reasons, there is a growing trend toward using industrial by-products as supplementary materials in the production of different types of concrete mixtures. Among the various supplementary materials, fly ash (FA) is the most commonly available mineral admixture. This by-product from industrial processes is usually available in large quantities. However, in the past few years, FA has been used as a substitution of cement with regard to its application in ECC [11-13]. Higher concentration of cement is obtained when coarse aggregate is absent in ECC. Furthermore, partial replacement with FA helps to reduce ecological loadings. As mentioned previously, employing larger quantities of mineral admixtures, particularly FA, helps decreasing the strength of matrix while enhancing that of ECC with respect to tensile ductility [13-15]. Moreover, anhydrite mineral admixtures having small particle size and even spherical shape are employed as filler particles, providing higher density of the fibre/matrix interface transition zone resulting to produce high frictional bonding. This enhances long-term stability of the structure by significantly decreasing the steady-state crack width.

It is hypothesized that the increase in matrix toughness due to an increased amount and size of aggregates could potentially be offset by the decrease in toughness when high-volume mineral admixture is used in the production of ECC. Recently, Sahmaran et al.[16, 17] investigated the influence of aggregate size on the mechanical properties of high-volume FA-ECC. The test results indicate that aggregates with a maximum aggregate size of up to 2.38 mm, as long as they do not interfere with the uniform fiber dispersion, do not negatively influence the ductility of ECC. In addition to aggregate size, there is a desire to increase the amount of aggregates and explore the use of an alternative mineral admixture type beyond FA. However, far too little attention has been paid to study the flexural behavior of the ECC beams numerically. In addition, no research has been found that surveyed the influence of simultaneously increasing the aggregate amount and size on the tensile behavior and dimensional stability in terms of free and restrained shrinkage of ECC. This study intends to fill this knowledge gap.

The objective of this study is to investigate the influence of simultaneously increasing the aggregate amount and size on the flexural behavior of the ECC beams using 3D nonlinear finite element simulation by ANSYS software. The comparative analysis of these results with those obtained through experimental study of elements having similar geometric and mechanical characteristics, employing them as reference models. A nonlinear parametric study was conducted to examine the influence of the factors considered on the flexural stress and flexural deflection. Based on the results of the statistical study, a prediction model is proposed that considers the parameters that influence the flexural stress and flexural deflection of ECC beams. The proposed model includes the ECC aggregate content (*AC*), ECC compressive strength (f_{ECC}), and maximum aggregate size (D_{max}). In addition, a database of the results of tests on 57 ECC beams reported in the literature [16, 17] was assembled for use in verifying the accuracy of the proposed new model.

2. Numerical Modelling of ECC Beams

A. ANSYS Finite Element Models

ANSYS program was employed to determine the malfunctioning of nonlinear finite element model. The program is able to deal with the particular numerical models designed to account for the nonlinear course of actions of concrete and ECC beams operating under invariable loadings. The ECC beams and Microsilica concrete (MSC) were modelled by using SOLID 65 elements. Each of these elements entails eight nodes with three levels of freedom at each node and transformations in the nodal x-, y- and z-directions. SOLID 65 elements hold the properties of plastic deformation, three dimensional cracking and crushing. ANSYS employs linear isotropic and multi-linear isotropic material attributes for modelling concrete, along with supplementary concrete material properties, for replicating actual concrete behaviour [18].

The state of cracked surface is indicated through the shear transfer coefficient β_t, whose value ranges from 0.0 to 1.0, where 0.0 symbolizes a smooth crack while 1.0 represents a coarse crack [19, 20]. In this study, the value of shear transfer

coefficient of an open crack, β_t is 0.2 [21] while the value of shear transfer coefficient of a closed crack, β_c is 0.8 [22]. For ECC beams, β_t=0.05 and β_c=0.45, were adopted [23].

The equation $E_c = 4700\sqrt{f_c^{'}}$, can be used to calculate the modulus of elasticity of the MSC while the tensile strength can be computed from the equation $f_r = 0.62\sqrt{f_c^{'}}$. The Poisson's ratio gave the value of 0.2. Furthermore, the following equations for the multi-linear isotropic stress–strain curve were used to obtain the compressive uniaxial stress–strain values for the MSC model [21, 22]:

$$E_c = f_{el}/\varepsilon_{el}\,, \quad \varepsilon_o = \frac{2f_c^{'}}{E_c} \quad \text{and} \quad f = \frac{E_c\varepsilon}{1+(\varepsilon/\varepsilon_o)^2} \tag{1}$$

Where f_{el} is the stress at the elastic strain (ε_{el}) in the elastic range ($f_{el} = 0.30f_c^{'}$), ε_o is the strain at the ultimate compressive strength, $\sqrt{f_c^{'}}$ is the compressive strength of the concrete from tests on cylinders and f is the stress at any strain ε .

For ECC, typical stress-strain curves obtained from uniaxial tension and compression tests are shown as dotted lines in Fig. 1. The following equations were used to obtain the tensile stress-strain relationship of ECC [24]:

$$\sigma_t = \frac{\sigma_{tc}}{\varepsilon_{tc}}\varepsilon \qquad 0 \le \varepsilon < \varepsilon_{tc} \tag{2}$$

$$\sigma_t = \sigma_{tc} + (\sigma_{tu} - \sigma_{tc})\left(\frac{\varepsilon - \varepsilon_{tc}}{\varepsilon_{tu} - \varepsilon_{tc}}\right) \qquad \varepsilon_{tc} \le \varepsilon < \varepsilon_{tu} \tag{3}$$

Where σ_{tc} represents the first cracking strength in tension, ε_{tc} represents the strain at first cracking, σ_{tu} represents the ultimate tensile strength, ε_{tu} represents the tensile strain at σ_{tu} .

The compressive stress-strain relationship of ECC can be expressed as [24]:

$$\sigma_c = 2\frac{\sigma_{c0}}{\varepsilon_{c0}}\varepsilon \qquad 0 \le \varepsilon < \frac{1}{3}\varepsilon_{c0} \tag{4}$$

$$\sigma_c = \frac{2}{3}\sigma_{c0} + \frac{\sigma_{c0}}{2\varepsilon_{c0}}\left(\varepsilon - \frac{\varepsilon_{c0}}{3}\right) \qquad \frac{1}{3}\varepsilon_{c0} \le \varepsilon < \varepsilon_{c0} \tag{5}$$

$$\sigma_c = \sigma_{c0} + (\sigma_{cu} - \sigma_{c0})\left(\frac{\varepsilon - \varepsilon_{c0}}{\varepsilon_{cu} - \varepsilon_{c0}}\right) \qquad \varepsilon_{c0} \le \varepsilon < \varepsilon_{cu} \tag{6}$$

where σ_{c0} represents the compressive strength, ε_{c0} represents the strain at peak stress, σ_{cu} represents the ultimate compressive stress (in the postpeak branch), ε_{cu} represents the ultimate compressive strain.

In this study, $\sigma_{cu} = 0.5\sigma_{c0}$ and $\varepsilon_{cu} = 1.5\varepsilon_{c0}$ were adopted. The maximum size of the concrete elements was taken as 1×1×1 mm.

The PVA fibres were modelled by using Link 8 elements. This is a 3D spar element having two nodes and three levels openings at each node. It holds the property of plastic deformation [18]. In this study, bond between the concrete and the PVA fibres is considered as effective as that between nodes of corresponding concrete solid elements. This helps to bring the same nodes to share same material. As per the finite element model, the fibres were considered as bilinear, isotropic, elastic and perfectly plastic material. A value of 0.42 was used for the poisson's ratio.

Solid 185 element [18] were used to model the loading and support plates. The solid element has eight nodes with three degrees of freedom at each node, translations in the nodal x, y, and z directions. The steel plates incorporated into the finite element models were assumed to be linearly elastic materials with an elastic modulus of 200 GPa and a poisson's ratio of 0.3.

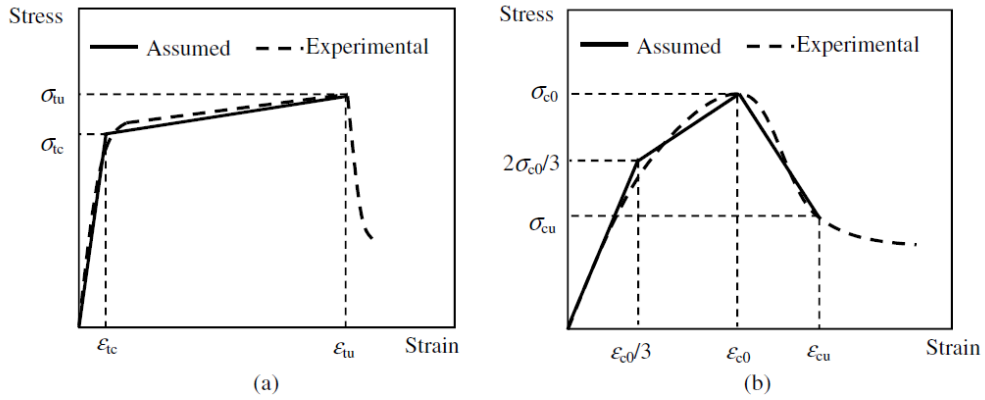

Figure 1: Stress-strain relationship of ECC. (a) Under uniaxial tension; (b) under uniaxial compression.

B. Structural Models

In order to study the flexural behaviour of ECC beams, six ECC beams with dimensions of (360×75×50) mm, have been modelled and compared with MSC beam model, as shown in Fig. 2. The beams were designed to be simply supported over a clear span of 304 mm and subjected to four-point loading. The basic mixture ingredients in ECC were: two different fine aggregate sizes (400 and 1000) µm, three aggregate contents (0.36, 0.45, and 0.55 A/B), Fly ash (FA) mineral admixture type, (2.2 FA/C ratio) mineral admixture replacement rate and a constant water-binder ratio (*w*/*b*) of 0.27 are considered. Details of this factorial design and designation of mixtures are presented in Table 1. PVA fiber 8 mm in length and 39µm in diameter extensively used in this study. To account for material inhomogeneity, a PVA fiber content of 2% by volume has been typically used in the mixture design. Table 2 illustrates the mechanic and geometric properties of PVA fibers. All the used data in this study based on confirmed experimental results, which have been achieved by [25].

3. Verification of Numerical Modelling with Experimental Results

A. Load-Deflection Curves

The flexural load-midspan beam deflection curves for all the ECC beams are shown in Fig. 3. In the flexural load-deflection curves, the load at the first drop associated with the first cracking is defined as the first cracking load, the maximum load is defined as the flexural load, and the corresponding deflection is defined as the flexural deflection (midspan beam deflection) capacity.

Fig. 3 further shows that while operating under deflecting load, an ECC beam having maximum size of 1000 µm bends similar to that of a ductile metal plate due to its property of plastic deformation. In all ECC beams, the flexural cracks prevailing at the tension surface are the first cracks to appear. Following this, the load increases along with producing multiple cracking, enhancing the inelastic deformation with an increase in stress. Microcracks produced from the first cracking point continued to extend in the midspan of the flexural beam. However, upon reaching the certain limit of fibre strength of the microcracks, bending failure in ECC took place, leading to cause a particular extent of deflection in that part when it reached its limit of flexural strength.

The average first-crack load of ECC beam varies from 780 to 1120 N in accordance with maximum aggregate size. The increase in the maximum aggregate size from (400 to 1000) µm reduces the first-crack load by an average of up to 44%. However, aggregate amount has little or no influence on the magnitude of the first-crack load of the ECC beams. Also, the stiffness of the beams does not appear highly sensitive to maximum aggregate size at a given aggregate content. This result is consistent with what is stated in the previous researches [26-28].

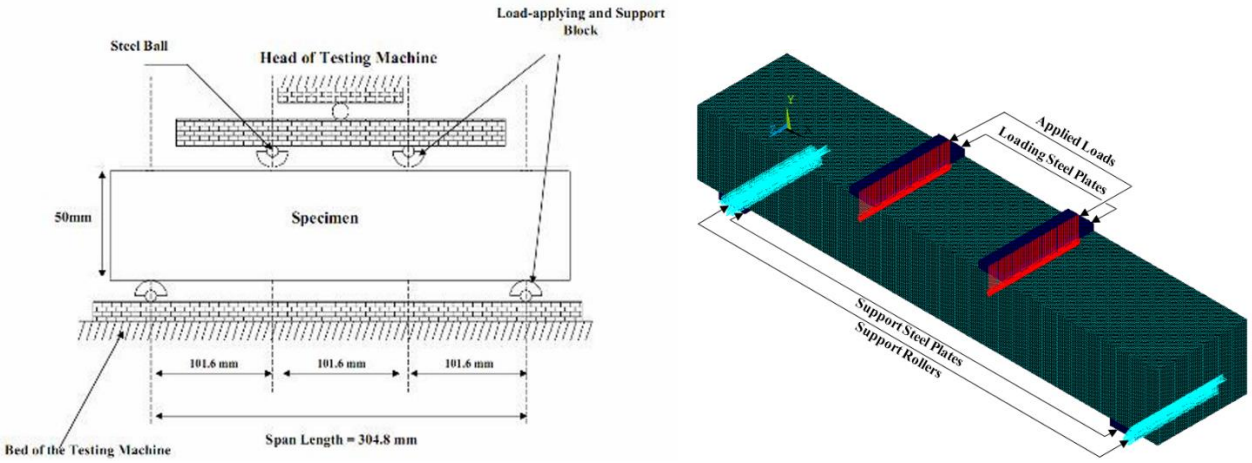

(a) (b)

Figure 2: Experimental and numerical specimens. (a) four-point bending test; (b) 3 dimensional model.

Table 1: ECC mixture proportions containing fly ash by weight.

Specimen ID.	Cement	*w/b*	Aggregate/Binder		FA/C	HRWR (kg/m^3)
			0-400 µm	0-1000 µm		
FA-2.2-0.36-400	1	0.27	0.36	-	2.2	3.0
FA-2.2-0.45-400	1	0.27	0.45	-	2.2	3.0
FA-2.2-0.55-400	1	0.27	0.55	-	2.2	3.0
FA-2.2-0.36-1000	1	0.27	-	0.36	2.2	3.0
FA-2.2-0.45-1000	1	0.27	-	0.45	2.2	3.0
FA-2.2-0.55-1000	1	0.27	-	0.55	2.2	3.0

Table 2: Mechanical and geometric properties of PVA fibres.

Fiber Type	Nominal Strength (MPa)	Apparent Strength (MPa)	Diameter (µm)	Length (mm)	Young Modulus (GPa)	Strain (%)	Specific Weight (kg/m^3)
PVA	1620	1092	39	8	42.8	6.0	1300

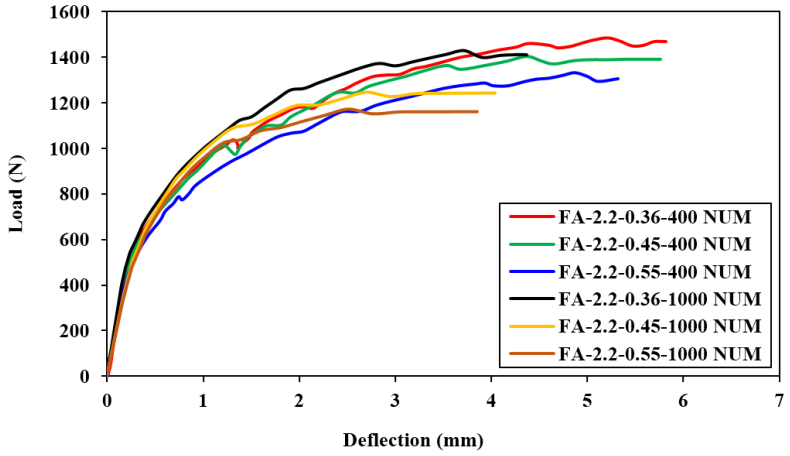

Figure 3: Numerical flexural load-deflection curves of ECC beams.

B. Flexural Strength

The numerical flexural strength data for all the beams studied and clarified in Fig. 4. The predicted stress values firstly increase linearly with corresponding deflection before yield strength of 7.42 MPa for 400 µm maximum aggregate size beams and 9.75 MPa for 1000 µm maximum aggregate size beams. After that, the curve suddenly changed and keeps almost horizontal until ultimate moment capacity is reached.

Fig. 4 further shows that the averaged ultimate flexural strengths vary from 9.62 to 10.93 MPa for numerical results. The increase in the maximum aggregate size from (400 to 1000) µm reduces the ultimate flexural stress by an average of up to 14%. As in the case of compressive strength results, the aggregate content and maximum aggregate size also appear to have a negligible effect on the flexural strength, at least within the parametric range investigated in experimental and numerical studies.

The similarity between the simulation and practical results can be illustrated through the Fig. 5. The average ultimate strength from the numerical simulation for (400 and 1000) µm maximum aggregate size beams are slightly larger than those from the experimental results (1.3%). This indicates that there is a good agreement between the numerical and experimental results. Also the results showed that the increase in the aggregate content reduces the ultimate flexural stress in accordance with the maximum aggregate size which match the experimental results.

It is evident that the stresses of beam are decreased by the increase in aggregate content and maximum aggregate size as per the contour plots of the simulation results of flexural stress shown in Fig. 6. The cracks continued to spread over the top layer of the beam after cracking, without noticeable crack width. The constant moment region was also surrounded by various minute cracks with parallel to the major one. At the same time, amid the loading process the division of various minute cracks is also starting from the centre to both supports of the beams. After initial cracking, several cracking along the specimens and minor strain hardening behaviour is quite evident. Following that, the external moment causes to distort the adhering of fibres and cementitious matrix reducing their ability to withstand the tensile stresses. In this stage the load was continues to decrease gradually once the maximum load is applied. In the end, the ECC beams failed to sustain the stress, leading to cause multiple fibre fracture, giving rise to major cracks in the midspan.

It appears from Fig.7 that the ECC beams show enhancement in terms of flexural stress when compared with MSC beam. The average percentage strength improvement of 400 µm maximum aggregate size ECC beams from numerical and experimental results as compared to that of MSC beam were 49.22% and 48.19%, respectively. While for 1000 µm maximum aggregate size ECC beams, the average enhancement percentage in flexural stress were 40.93% and 38.14% based on numerical and experimental results, respectively.

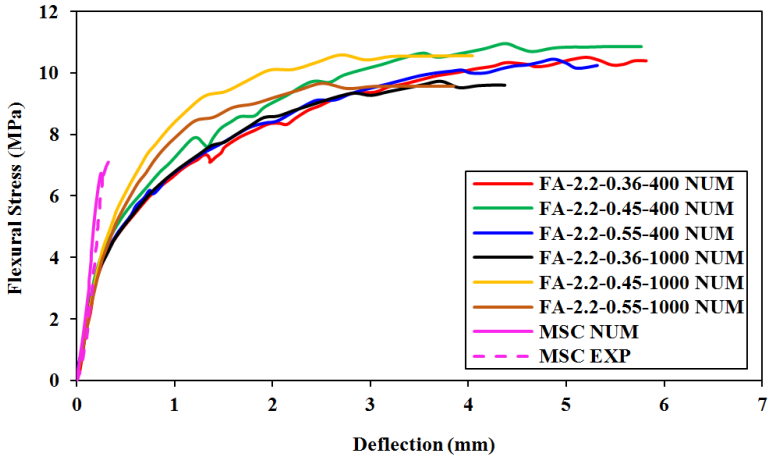

Figure 4: Comparison between numerical and experimental flexural stress-deflection curves of ECC and MSC beams.

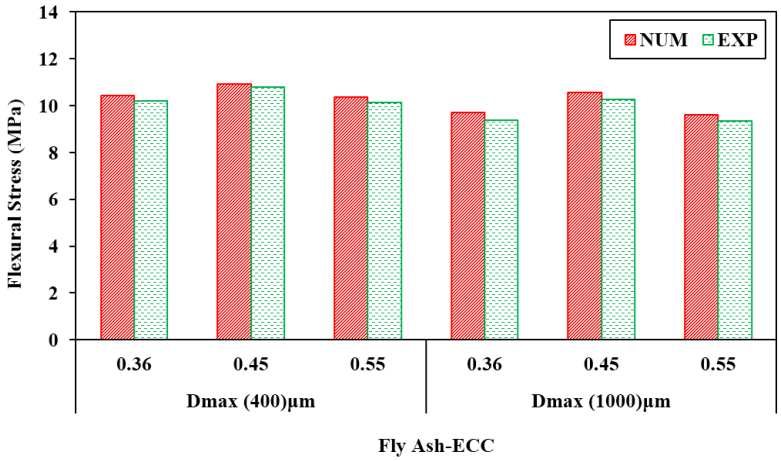

Figure 5: Comparison between numerical and experimental influence of aggregate size and amount on flexural stress.

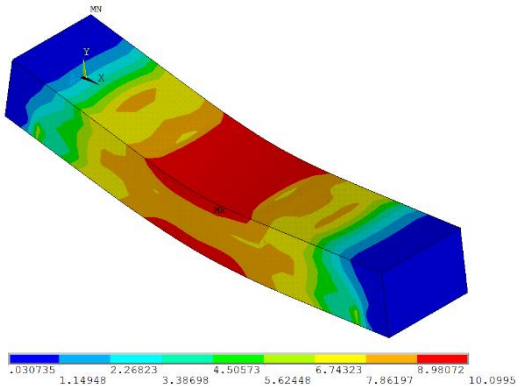

(a) AC=0.36, D_{max}=400

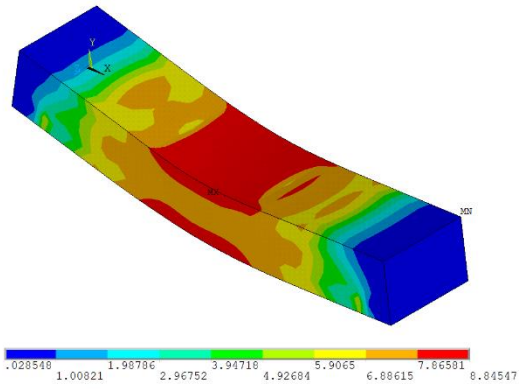

(b) AC=0.36, D_{max}=1000

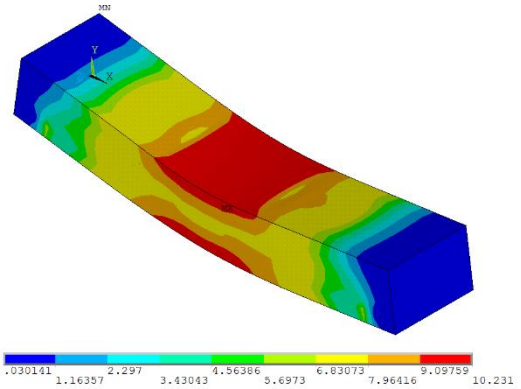

(c) AC=0.45, D_{max}=400

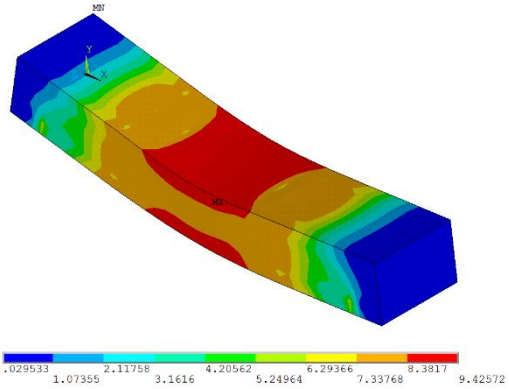

(d) AC=0.45, D_{max}=1000

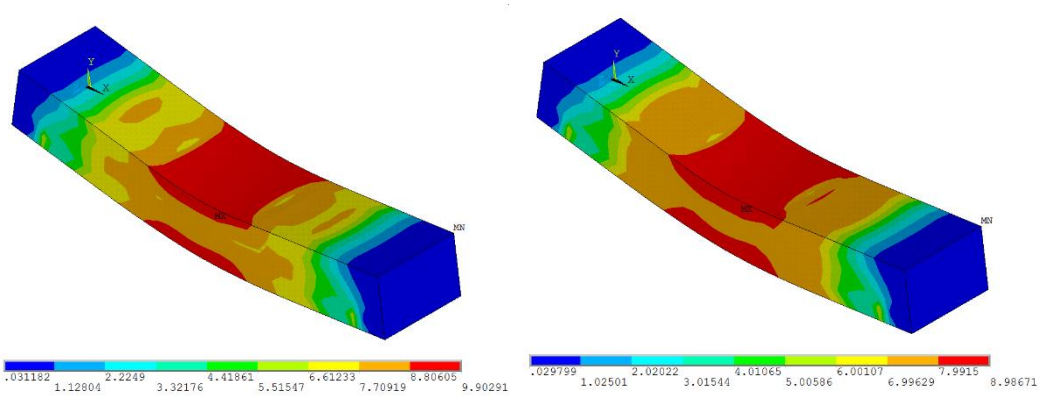

(e) AC=0.55, D_{max}=400 (f) AC=0.55, D_{max}=1000

Figure 6: Contour plots of flexural stress for ECC beams.

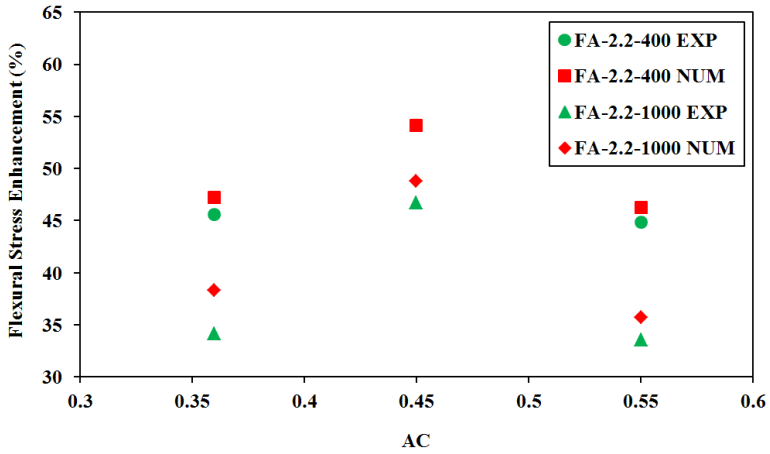

Figure 7: Flexural stress enhancement versus aggregate content of numerical and experimental results for ECC beams.

C. Flexural Strain

A normal numerical flexural stress– strain curve is shown in Fig. 8, which can be parted into two sections:

1. Elastic stage: This occurs along the first cracking process. The point of first cracking is analogous to the end of the initial linear section of the stress–strain curve. The strain at this stage is called first cracking strain.
2. Strain hardening stage: In this stage the flexural load-carrying ability increases to cause a consequent increase in strain which is accompanied by multiple cracking. The strain at this stage is called flexural strain.

The average ultimate strain for (400 and 1000) µm maximum aggregate size ECC beams are 1417% and 1067% higher than that from MSC beam, respectively. As seen from Fig. 9, the maximum strain and deflection decrease with an increase in aggregate content of 400 µm maximum aggregate size ECC beams by percentage of 10.34% and 9.21%, respectively and 13.64%, 12.24%, respectively, for 1000 maximum aggregate size ECC beams. Fig. 10 illustrated the contour plots of the simulation results of flexural strain for ECC beams, where, the increase in the maximum aggregate size from (400 to 1000) µm reduces the maximum flexural strain by an average of up to 22%. Specifically, high aggregate content and the presence of coarse aggregates in a paste tend to increase the matrix (ECC without fiber) toughness, which delays crack initiation and prevents steady-state flat-crack propagation, resulting in a loss of tensile ductility of ECC. Furthermore, employing aggregates having a particle size larger than the average fibre spacing may cause balling of fibres, leading to provide inadequate fibre dispersion uniformity [8, 9].

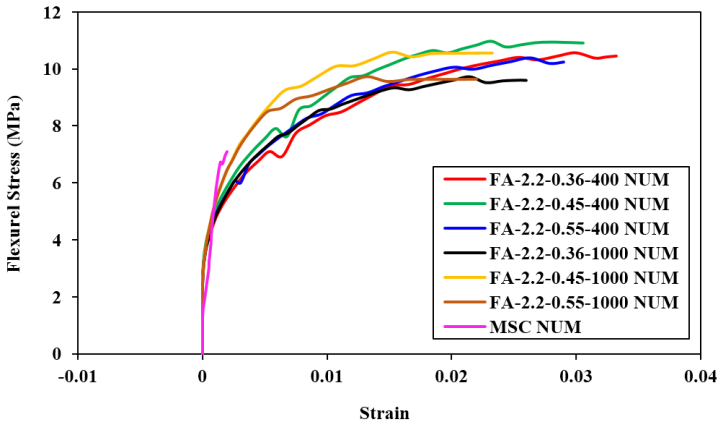

Figure 8: Numerical flexural stress-strain curves of ECC and MSC beams.

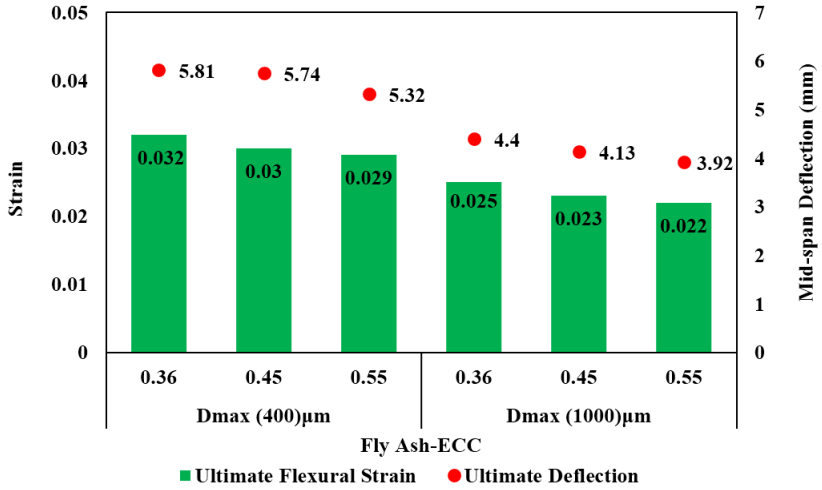

Figure 9: Influence of aggregate size and content on the flexural strain and deflection.

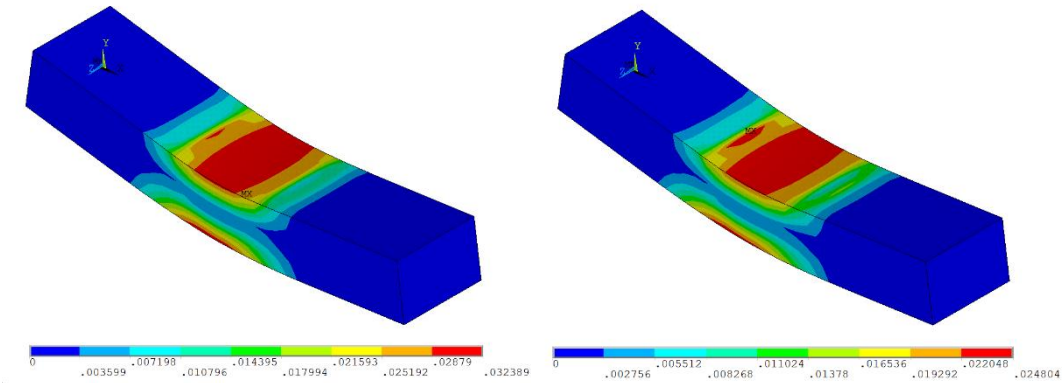

(a) AC=0.36, D_{max}=400 (b) AC=0.36, D_{max}=1000

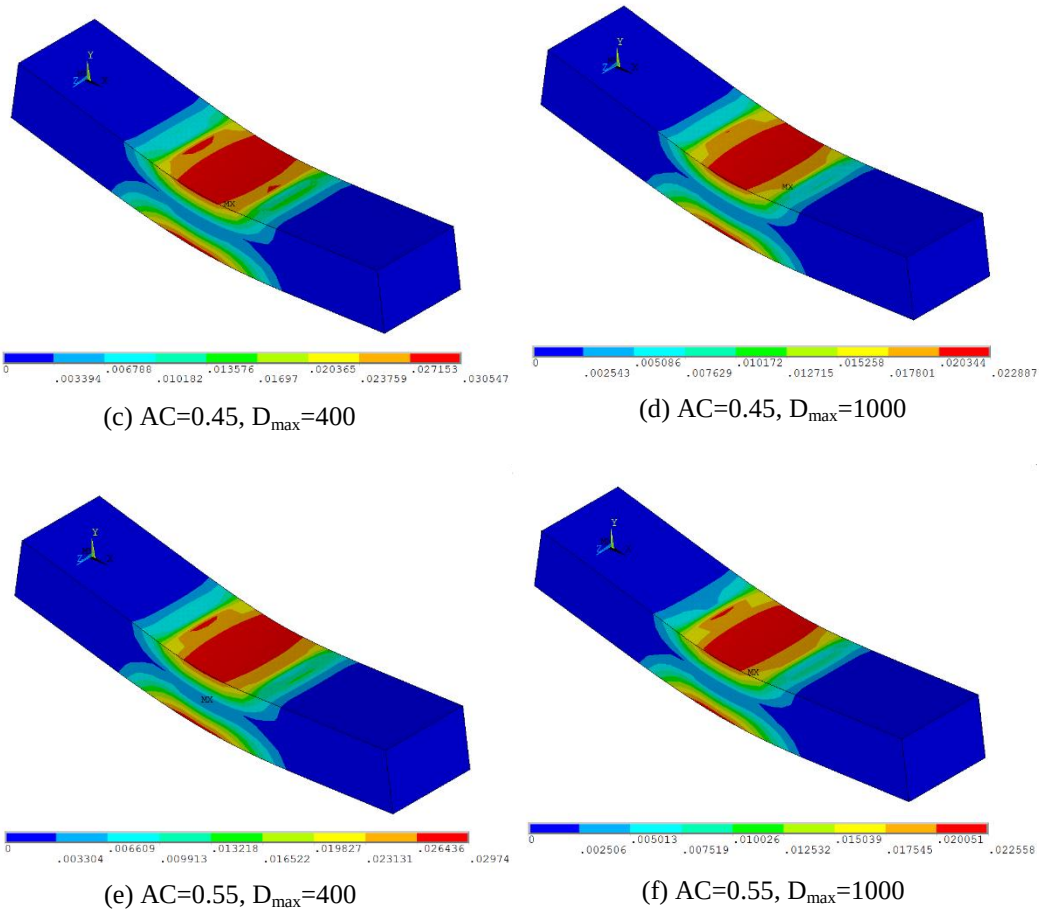

(c) AC=0.45, D_{max}=400

(d) AC=0.45, D_{max}=1000

(e) AC=0.55, D_{max}=400

(f) AC=0.55, D_{max}=1000

Figure 10: Contour plots of flexural strain for ECC beams.

D. Mid-span Beam Deflection

The flexural deflection capacity of ECC beams, which reflects the material ductility, is summarized in Fig. 11. As shown in this figure, the total deflection of the ECC beam strongly depends on the type and amount of mineral admixture. Beams of FA-ECC showed significantly good deflection capacity when compared to the MSC beam. The improvement in the deflection capacity with the use of FA can be attributed to the fact that the addition of FA has a tendency to reduce PVA fiber/matrix interface chemical bond and matrix (ECC without fiber) toughness while increasing the interface frictional bond [29]. Also, the similarity between the numerical and experimental results can be illustrated through the Fig. 11, where, the average ultimate deflection from the numerical simulation for (400 and 1000) μm maximum aggregate size beams are slightly higher than those from the experimental results with 1.4% variation.

The adverse effects of increased size of aggregates on ductility performances of ECC are shown in Fig. 11. This figure indicates that the increase in aggregate size and amount result in a decrease in the ECC ductility. The negative effects of increasing aggregate size at large aggregate content on ductility may be attributed to the corresponding poor dispersion of fibers. Required coating of fibres by the matrix is avoided by the balling of fibres supported by coarser aggregates at continuous aggregate content. Therefore, this affects a significant component that affects ductility i.e. effective fibre content [9]. In addition, a greater extent of aggregate interconnection is anticipated for ECCs with larger aggregate size and volume, giving out a greater matrix toughness, which results in the decrease in the margin to develop multiple cracking.

It appears from Fig.12 that the ECC beams show enhancement in terms of deflection when compared with MSC beam. The average percentage deflection improvement of 400 μm maximum aggregate size ECC beams from numerical and experimental results as compared to that of MSC beam were 1657.3% and 1714.2%, respectively. While for 1000 μm maximum aggregate size ECC beams, the average enhancement percentage in deflection were 1197% and 1185% based on numerical and experimental results, respectively.

Other than ECC properties, characteristics and kinds of mineral admixture plus amount of the PVA fibres also determine the flexural behaviour of the beam specimens. Nonetheless, appropriate and suitable estimates of experimental outcomes can be provided by the simulation outcomes. It is to be noted that the techniques that are used to examine the flexural behaviour of the ECC are tested before they are implemented. The suggested numerical mechanism will be employed to evaluate the impacts of various parameters on the mechanical behaviour of the ECC beams.

4. Nonlinear Parametric Study

A nonlinear parametric study is carried out to evaluate the influence of parameters on the prediction of the flexural stress and flexural deflection of ECC beams in a 3D FE simulation, which comprises ECC aggregate content (*AC*), and ECC compressive strength (f_{ECC}) based on maximum aggregate size (D_{max}). These parameters have been obtained using an exponential regression line. The exponential regression analysis resulted in higher R^2 values (0.98) than other types of regression. This type of regression was used because it yielded a more realistic prediction of the flexural behavior of ECC beams. To examine the reliability and validity of the proposed new model, an extensive verification is carried out using a series of experimental data available in the literature [16, 17].

A. Influence of ECC Aggregate Content

The aggregate content is an important factor in the stiffness of the ECC beams. Fig. 13 illustrate the influence of the aggregate content on the likelihood of flexural stress, where, an increase in the aggregate content decreases the flexural stress of (400 and 1000) µm maximum aggregate size ECC beams by $10.571e^{-0.035AC}$ and $9.888e^{-0.049AC}$, respectively. Furthermore, the flexural deflection of (400 and 1000) maximum aggregate size ECC beams decreases with an increase in aggregate content by $6.923e^{-0.46AC}$ and $5.466e^{-0.61AC}$, respectively, as shown in Fig. 14.

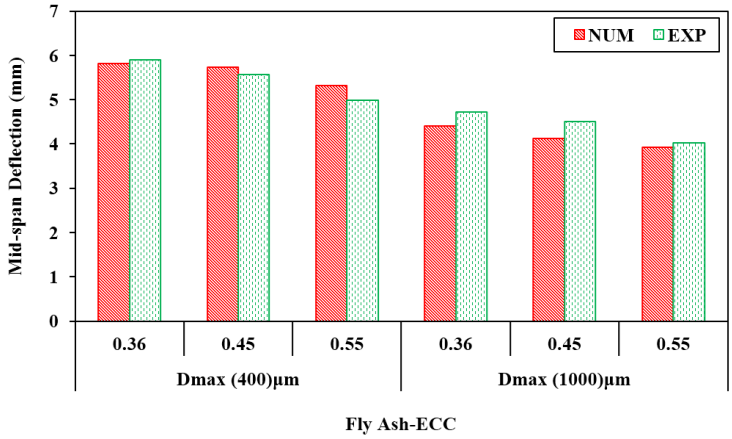

Figure 11: Comparison between numerical and experimental influence of aggregate size and amount on deformability in flexure.

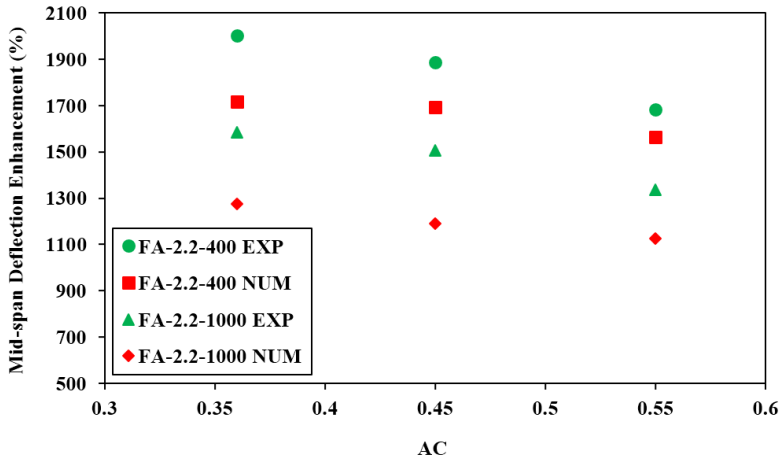

Figure 12: Deflection enhancement versus aggregate content of numerical and experimental results for ECC beams.

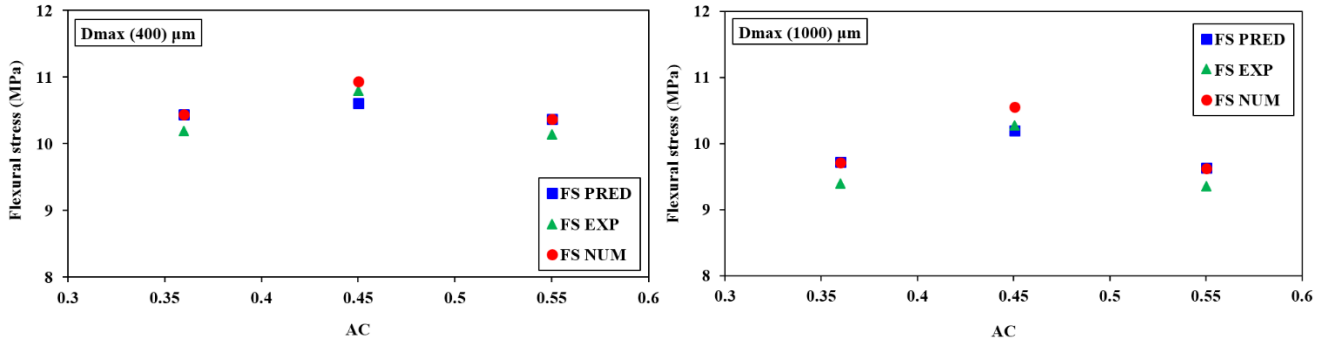

(a) (b)

Figure 13: Influence of aggregate content on the flexural stress by comparing experimental, numerical, and predicted results of ECC beams for: (a) 400 µm D_{max}; and (b) 1000 µm D_{max}.

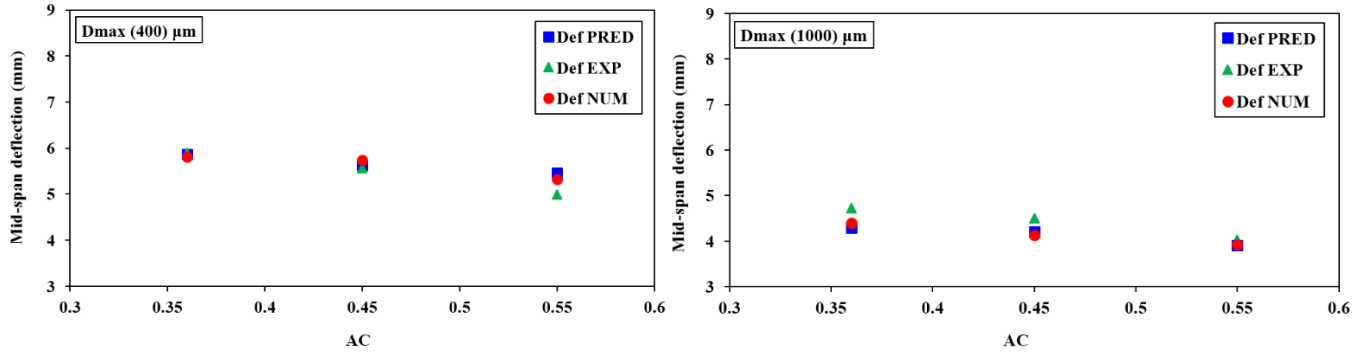

(a) (b)

Figure 14: Influence of aggregate content on the deformability in flexure by comparing experimental, numerical, and predicted results of ECC beams for: (a) 400 µm D_{max}; and (b) 1000 µm D_{max}.

B. Influence of ECC Compressive Strength

The compressive strength is also an important factor in the stiffness of the ECC beams. Fig. 15 clarify the influence of the compressive strength on the likelihood of flexural stress, where, an increase in the compressive strength increases the flexural stress of (400 and 1000) µm maximum aggregate size ECC beams by $11.69e^{-0.002f_{ECC}}$ and $2.031e^{0.032f_{ECC}}$, respectively. Furthermore, the flexural deflection of 400 µm maximum aggregate size ECC beams increases with an increase in compressive strength by $36.99e^{-0.04f_{ECC}}$ and decreases with an increase in compressive strength by $31.353e^{-0.04f_{ECC}}$ for 1000 µm maximum aggregate size ECC beams, as shown in Fig. 16.

C. Prediction of New Models

It is a well agreed notion that an ideal design of the ECC mixture having its factors in accordance with the micromechanical design theory necessarily requires to be an effective tool able to enhance the mechanical characteristics of hardened mixtures. Nevertheless, few studies are to be found providing detailed information and accurate correlations for describing the mechanical behaviour of ECC beams at present study conditions. Therefore, new correlations have been predicted to evaluate the ultimate flexural stress (*FS*) and ultimate flexural deflection (*Def*) statically depending on three parameters of ECC aggregate content (*AC*), ECC compressive strength (f_{ECC}), and maximum aggregate size (D_{max}), as shown in Eqs. (7) and (8):

$$FS = \frac{0.848AC^{-0.026}D_{\max}^{-0.098}}{f_{ECC}^{-0.628}} \tag{7}$$

$$Def = \frac{7.069AC^{-0.219}D_{\max}^{-0.321}}{f_{ECC}^{0.182}} \tag{8}$$

The experimental data provided in the literature was employed to test the validity and constancy of the newly presented model. The database considered consists of the results of 57 ECC beams. The main geometric and mechanical characteristics of the collected experimental data are close to the present study data. The predictions obtained with the proposed new model for the validation data set with predictions data of current study have been illustrated in both Figs. 17 and 18 for maximum flexural stress and deflection consecutively. The standard deviation values of FS_{Exp}/FS_{Pred} and Def_{Exp}/Def_{Pred} are 0.09, 0.15, respectively, and the mean values are 1.05, 1.09, respectively, the corresponding coefficients of variation (COV_S) are 8.57%, 13.76%, respectively, and the coefficients of correlation, R, are 0.98, 0.96, respectively. These values show that, from a statistical perspective, the proposed models are equally reliable for all of the ECC beams configurations considered in the analysis. Also, these figures include two lines that indicate a ± 11% and ±12% band about the mean new models prediction and include the reported experimental values for flexural stress and deflection results, respectively. It can be seen that most of the results fall within these bounds, and the average values of the new predicted models are found to be very similar to the experimental results.

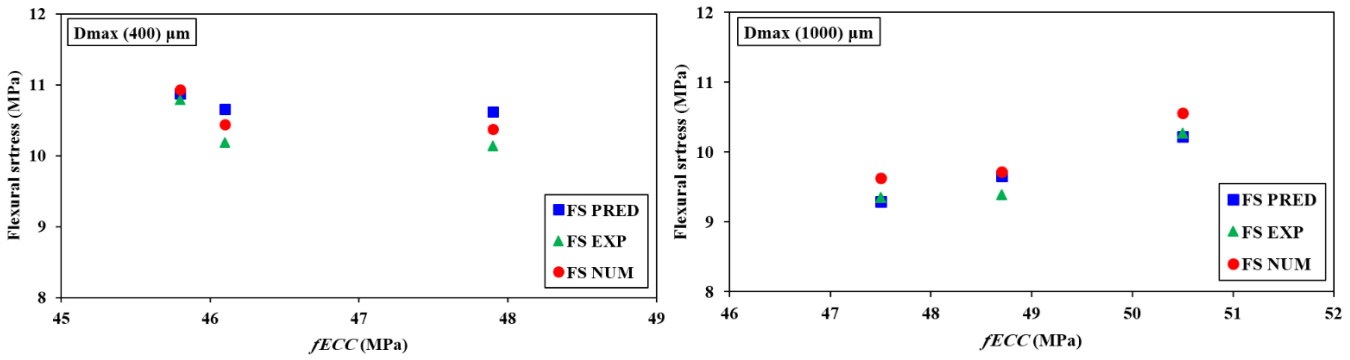

(a) (b)

Figure 15: Influence of ECC compressive strength on the flexural stress by comparing experimental, numerical, and predicted results of ECC beams for: (a) 400 µm D_{max}; and (b) 1000 µm D_{max}.

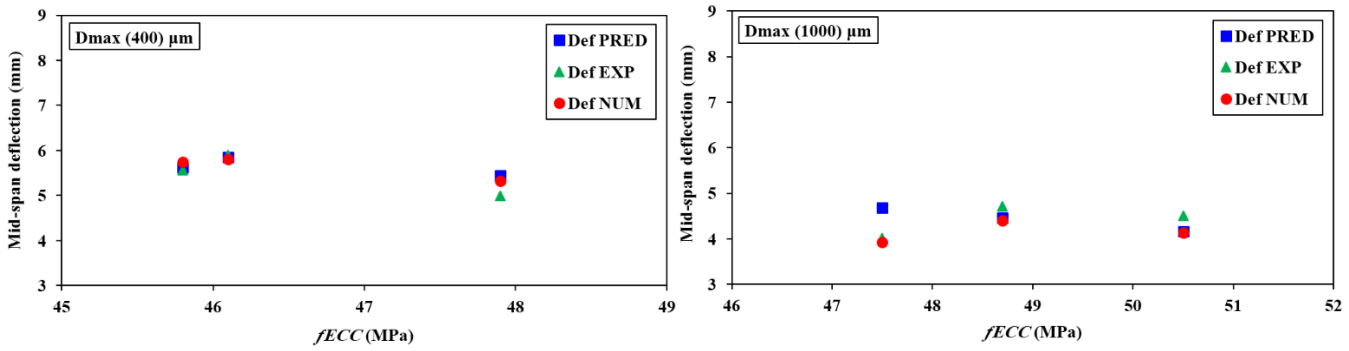

(a) (b)

Figure 16: Influence of ECC compressive strength on the deformability in flexure by comparing experimental, numerical, and predicted results of ECC beams for: (a) 400 µm D_{max}; and (b) 1000 µm D_{max}.

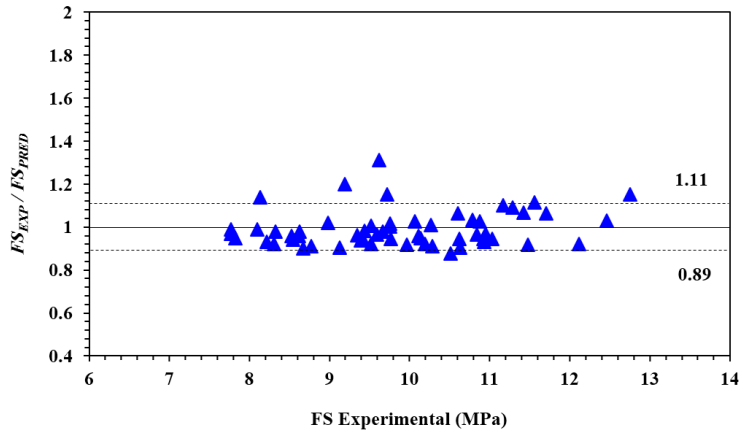

Figure 17: Predicted flexural stress by the new model in comparison with the experimental values.

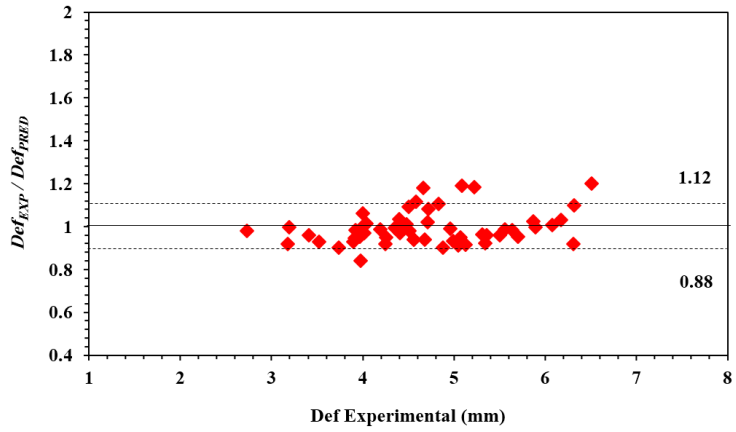

Figure 18: Predicted deflection by the new model in comparison with the experimental values.

5. Conclusions

This research aims to analyse the potential effect of aggregate size and amount upon the mechanical performances of ECC beams by means of employing nonlinear finite element model. To test the validity of models of the ECC beams operating under monotonic loading, experimental results were obtained. Based on the numerical analysis method, nonlinear parametric study was then conducted to evaluate the influences of various parameters on the flexural stress and flexural deflection of ECC beams. A new models that accounts for the ECC aggregate content (*AC*), ECC compressive strength (f_{ECC}), and maximum aggregate size (D_{max}) parameters are proposed. The analytical results obtained from the proposed models were compared with experimental results obtained from 57 ECC beam tests reported in the literature. From the results obtained, the following conclusions can be drawn:

- The simulation results indicate that when increase the aggregate size and content no definite trend in flexural strength is observed, at least for the limited aggregate size range studied. The ductility of ECC is negatively influenced by the increase of aggregate size and content.
- The ECC beams showed enhancement in terms of flexural stress, strain, and midspan deflection when compared with MSC beam, where, the average improvement percentage of the specimens were 45%, 1242%, and 1427.15%, respectively.
- As per the finite element analysis, the flexural stress- deflection property of the beams was in agreement with the results obtained from experiments. Nonetheless, the numerical values for average ultimate strength and deflection obtained for the beams are 1.3% and 1.4% larger than those obtained from the experimental results, respectively. In addition to the ECC properties, the flexural behaviour of the beam can also be identified through properties and nature of mineral admixture, and quantity of the PVA fibres. The accuracy of experimental results can only be obtained through replication of results. Furthermore, the numerical method to identify the flexural behaviour of the ECC beams is validated through these results.
- The nonlinear parametric study demonstrated that the mid-span beam deflection properties, through which material ductility, and flexural stress of ECC beams is indicated, are subjected to considerable variations with respect to changes in *AC* and f_{ECC} parameters. The deflection ability and flexural stress of the beams are in a negative relation with both of these factors.
- Based on the comparisons with the experimental results, the proposed model is more accurate in predicting the flexural behaviour of the ECC beams. The mean values of FS_{Exp}/FS_{Pred} and Def_{Exp}/Def_{Pred} are 1.05, 1.09 respectively. The corresponding coefficients of variation are 8.57%, 13.76%, respectively, and the coefficients of correlation are 0.98, 0.96, respectively. The error associated with predicting the flexural behaviour was less than 11% and 12%, respectively.

ACKNOWLEDGEMENT

The researchers gratefully acknowledge the technical support provided by Faculty of Civil Engineering at University of Gaziantep.

REFERENCES

[1] Fraternali, F., et al., Experimental study of the thermo-mechanical properties of recycled PET fiber-reinforced concrete. Composite Structures, 2011. 93(9): p. 2368-2374.

[2] Li, V.C., Engineered Cementitious Composites - Tailored Composites Through Micromechanical Modeling. Fiber Reinforced Concrete: Present and the Future edited by N. Banthia, in Fiber Reinforced Concrete: Present and the Future edited by N. Banthia, A. Bentur, A. and A. Mufti, Canadian Society for Civil Engineering, Montreal, 1998: p. 64-97.

[3] Lin, Z., T. Kanda, and V.C. Li, On interface property characterization and performance of fiber reinforced cementitious composites. Concrete Science and Engineering, 1999. 1(3): p. 173-184.

[4] Maruta, M., et al., New high-rise RC structure using pre-cast ECC coupling beam. Concrete Journal, 2005. 43(11): p. 18-26.

[5] Li, V.C., D.K. Mishra, and H.-C. Wu, Matrix design for pseudo-strain-hardening fibre reinforced cementitious composites. Materials and Structures, 1995. 28(10): p. 586-595.

[6] Li, V.C., S. Wang, and C. Wu, Tensile strain-hardening behavior of polyvinyl alcohol engineered cementitious composite (PVA-ECC). ACI materials Journal, 2001. 98(6).
[7] Dhawale, A. and V. Joshi, Engineered cementitious composites for structural applications. International journal of application or Innovation in Engineering & Management, 2013. 2: p. 198-205.
[8] De Koker, D. and G. Van Zijl. Extrusion of engineered cement-based composite material. in Proceedings of the 6th RILEM Symposium on Fiber-Reinforced Concretes (FRC). 2004. Citeseer.
[9] Parviz soroushian, M.N. and A.M. Jer-Wen Hsu, Optimization of the use of lightweight aggregates in carbon fiber reinforced cement. ACI Materials Journal, 1992. 89(3).
[10] Fischer, G. and V.C. Li, Deformation behavior of fiber-reinforced polymer reinforced engineered cementitious composite (ECC) flexural, members under reversed cyclic loading conditions. Aci Structural Journal, 2003. 100(1): p. 25-35.
[11] Kim, J.-K., et al., Tensile and fiber dispersion performance of ECC (engineered cementitious composites) produced with ground granulated blast furnace slag. Cement and Concrete Research, 2007. 37(7): p. 1096-1105.
[12] Zhou, J., et al., Development of engineered cementitious composites with limestone powder and blast furnace slag. Materials and Structures, 2010. 43(6): p. 803-814.
[13] Wang, S.X. and V.C. Li, Engineered cementitious composites with high-volume fly ash. Aci Materials Journal, 2007. 104(3): p. 233-241.
[14] Yang, D.S., S.K. Park, and K.W. Neale, Flexural behaviour of reinforced concrete beams strengthened with prestressed carbon composites. Composite Structures, 2009. 88(4): p. 497-508.
[15] Nematollahi, B., J. Sanjayan, and F.U. Ahmed Shaikh, Tensile Strain Hardening Behavior of PVA Fiber-Reinforced Engineered Geopolymer Composite. Journal of Materials in Civil Engineering, 2015: p. 04015001.
[16] Şahmaran, M., et al., Influence of aggregate type and size on ductility and mechanical properties of engineered cementitious composites. ACI Materials Journal, 2009. 106(3): p. 308-316.
[17] Şahmaran, M., et al., Improving the workability and rheological properties of Engineered Cementitious Composites using factorial experimental design. Composites Part B: Engineering, 2013. 45(1): p. 356-368.
[18] Manual, A.U.s., Version (15). Swanson Analysis Systems Inc, 2014.
[19] Kwan, A., H. Dai, and Y. Cheung, Non-linear seismic response of reinforced concrete slit shear walls. Journal of sound and vibration, 1999. 226(4): p. 701-718.
[20] Terec, L., T. Bugnariu, and M. Pastrav, Non-Linear Analysis of Reinforced Concrete Frames Strengthened with Infilled Walls. Revista Romana De Materiale-Romanian Journal of Materials, 2010. 40(3): p. 214-221.
[21] Damian, K., et al., Finite element modeling of reinforced concrete structures strengthened with FRP laminates. Report for Oregon Department Of Transportation, Salem, 2001.
[22] Raongjant, W. and M. Jing. Finite element analysis on lightweight reinforced concrete shear walls with different web reinforcement. in The Sixth Prince of Songkla Univ. Engng. Conf., Hat Yai, Thailand. 2008.
[23] Wolanski, A.J., Flexural behavior of reinforced and prestressed concrete beams using finite element analysis. 2004, Citeseer.
[24] Yuan, F., J. Pan, and C. Leung, Flexural behaviors of ECC and concrete/ECC composite beams reinforced with basalt fiber-reinforced polymer. Journal of Composites for Construction, 2013.
[25] Sahmaran, M., et al., Combined Effect of Aggregate and Mineral Admixtures on Tensile Ductility of Engineered Cementitious Composites. Aci Materials Journal, 2012. 109(6): p. 627-637.
[26] Cetin, A. and R.L. Carrasquillo, High-performance concrete: influence of coarse aggregates on mechanical properties. ACI Materials Journal, 1998. 95(3).
[27] Baalbaki, W., et al., Influence of coarse aggregate on elastic properties of high-performance concrete. ACI Materials Journal, 1991. 88(5).
[28] Aïtcin, P.-C. and P.K. Mehta, Effect of coarse aggregate characteristics on mechanical properties of high-strength concrete. ACI Materials Journal, 1990. 87(2).
[29] Li, V., From micromechanics to structural engineering – the design of cementitious composites for civil engineering applications. Struct Eng Earthq Eng Jpn Soc Civ Eng, 1993. 10(2): p. 37–48.